Coordination Chemistry Reviews, 21 (1976) 1—27

MAGNETIC INTERACTION IN METAL COMPLEXES WITH BRIDGING NITROGEN-HETEROCYCLIC LIGANDS

MOTOMICHI INOUE and MASAJI KUBO
Department of Chemistry, Nagoya University, Chikusa, Nagoya (Japan)
(Received 10 May 1976)

CONTENTS

A. INTRODUCTION

Diazoles, diazines, and other nitrogen heterocycles having two or more nitrogen atoms in a molecule have a potential capacity to coordinate, as "exobidentate ligands", on two different metal ions to form —M—L—M— links. The bridging type is characteristic of these nitrogen heterocycles in contrast with common "endobidentate ligands" such as 2,2'-bipyridine. Figure 1 shows some examples of various types of bridging exobidentate ligands as confirmed by X-ray crystal analysis. The —M—L—M— links give rise to dimeric clusters, chain molecules, and two- or three-dimensional network structures, all of which attract attention in relation to the electronic state of metal complexes including those of biological interest such as imidazole and purine complexes.

When —M—L—M— links are formed between paramagnetic ions, spin exchange interaction is expected to operate between the metal ions. Accordingly, complexes having bridging heterocyclic ligands present an interesting topic of magnetic interaction. The statistic theory of spin lattices has already been well advanced to formulate exactly the magnetic susceptibilities of simple clusters and one-dimensional lattices. It is now possible to discuss the energies of the spin interaction determined for crystals containing these spin aggregations in relation to other physical quantities observable in magnetic resonance,

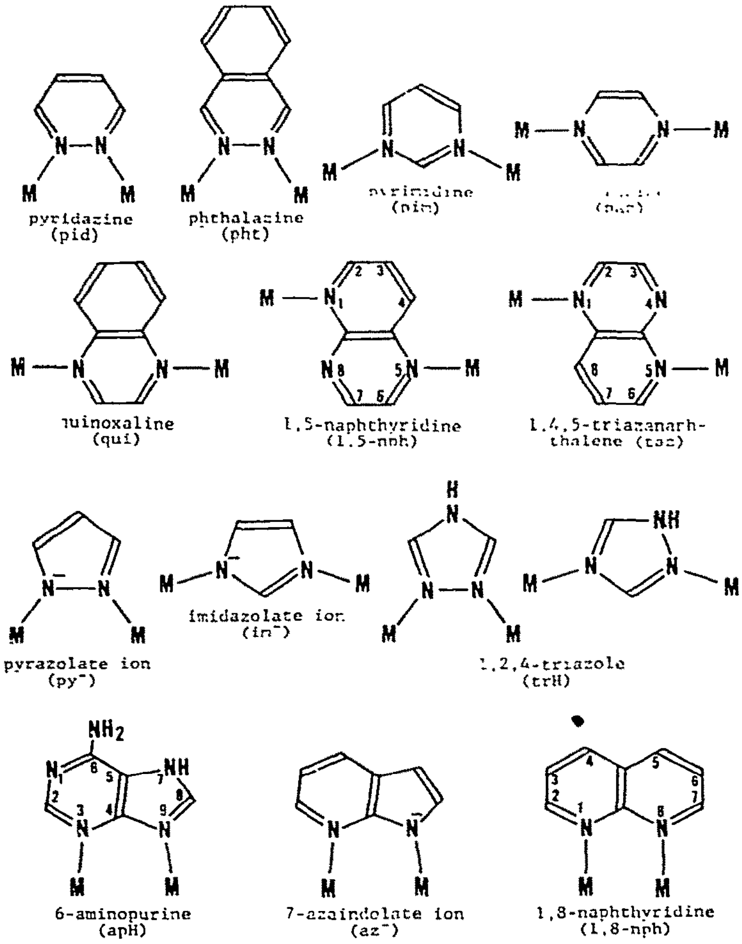

pyridazine (pid)
phthalazine (pht)
pyrimidine (pim)
(paz)
quinoxaline (qui)
1,5-naphthyridine (1,5-nph)
1,4,5-triazanaphthalene (taz)
pyrazolate ion (py⁻)
imidazolate ion (im⁻)
1,2,4-triazole (trH)
6-aminopurine (apH)
7-azaindolate ion (az⁻)
1,8-naphthyridine (1,8-nph)

Fig. 1. Examples of —M—L—M— links.

electronic spectra, etc. The spin exchange interaction is due to the delocalization of unpaired electrons in metal ions diffusing into ligand molecules or ions. Therefore, the mechanism of the interaction involves the electronic state of M—L bonds as well as of ligand molecules or ions as a whole. The effect of spin delocalization is revealed by Fermi contact shifts obtainable from proton magnetic resonance. Thus, the study of PMR provides valuable information for the elucidation of the mechanism of spin exchange interaction.

In this review, magnetic parameters evaluated from the temperature dependence of magnetic susceptibility are discussed to clarify the effect of bridging ligands on the exchange interaction energy by taking into account information on the mechanism of interaction obtained from the study of PMR.

B. EXAMPLES OF METAL—LIGAND—METAL LINKS

Although the formation of —M—L—M— links in diazole and diazine complexes had been suspected for a long time from chemical compositions, magnetic moments, IR and UV spectra, etc., it was mostly during the last decade that many structures were confirmed by X-ray crystal analysis.

Jarvis [1] carried out an X-ray analysis on a crystal of $CuCl_2(trH)$ and found that the coordination of exobidentate 1,2,4-triazole molecules leads to the formation of —M—N—N—M— links in the crystal as shown in Fig. 2. Each copper ion has a distorted octahedral coordination group consisting of four chloride ions at the corners of a slightly distorted square and two nitrogen atoms located above and below the plane of the square. Neighboring octahedral groups are joined by sharing Cl—Cl edges and are also linked by a 1,2,4-triazole molecule to form an infinite chain as a structural unit in the crystal. Reimann and Zocchi [2] report an interesting structure involving —Ni—N—N—Ni— links for $Ni(NO_3)_2(trH)_2 \cdot 8/3H_2O$. In this crystal, linear trinuclear cluster ions, $[(H_2O)_3Ni(trH)_3Ni(trH)_3Ni(H_2O)_3]^{6+}$, exist as structural units, neighboring nickel atoms being bridged by three 1,2,4-triazole molecules.

On losing a proton, an imidazole molecule (imH) acts as a uninegative exobidentate ligand. The X-ray crystal analysis of $Cu(im)_2$ [3,4] has shown the formation of —Cu(1)—(im)—Cu(2)—(im)—Cu(1)— chains in crystals. Each Cu(1) atom has a flattened tetrahedral coordination, whereas the Cu(2) atom has square coordination. The chains are kinked at Cu(1) atoms to give rise to a three-dimensional network structure. A preliminary X-ray analysis of $Zn(im)_2$ [4] has shown that each imidazolate ion is coordinated to two different zinc atoms to form a —Zn—(im)—Zn— link and that each zinc atom

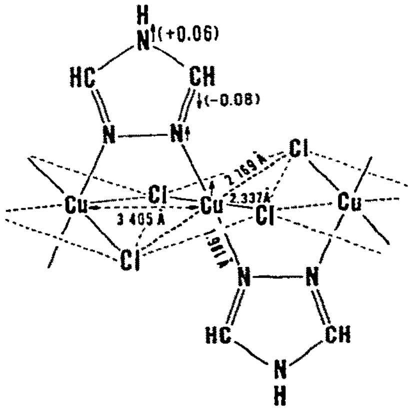

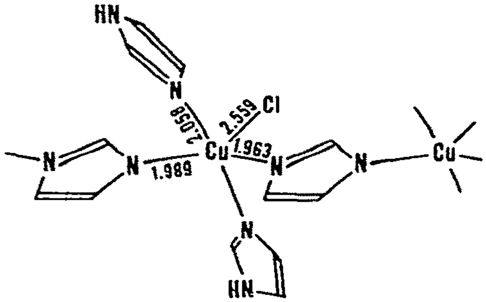

Fig. 2. Structure of $CuCl_2(trH)$ and spin densities on the ligand [1,56,97].

Fig. 3. Linear chain structure of $CuCl(im)(imH)_2$ [6].

has a tetrahedral coordination. Lundberg and co-workers [5,6] report that —Cu—(im)—Cu— links are formed in the crystals of $Cu_3(ClO_4)_4(im)_2(imH)_8$ and $CuCl(im)(imH)_2$. The former consists of linear trinuclear clusters, in which (imH) is unidentate whereas an (im) ion is a bidentate ligand forming a —Cu—(im)—Cu— link. The latter crystal contains one-dimensional infinite —Cu—(im)—Cu— chains having unidentate (imH) ligands as shown in Fig. 3.

The complexes MX_2(paz) of cobalt(II) or nickel(II) halides with pyrazine or its derivatives have been suspected from their electronic spectra, magnetic moments, and IR spectra to have a structure shown in Fig. 4(A) [7—9]. In this structure, metal atoms are bridged by halogen atoms to form linear chains of the same type as in $CoCl_2$(pyridine)$_2$ and $CuCl_2$(pyridine)$_2$ shown in Fig. 4(B) [10,11], and the resulting chains are crosslinked by exobidentate pyrazine molecules. The proposed structure has been confirmed by Ayres et al. [12], who have carried out X-ray crystal analysis on $NiBr_2$(2,5-dimethylpyrazine). Later, several examples of —M—(paz)—M— links have been reported. In a crystal of $Cu(NO_3)_2$(paz), infinite —Cu—(paz)—Cu— chains are formed as shown in Fig. 5 [13]. The shortest distance between copper atoms belonging to different chains amounts to as much as 5.142 Å, suggesting the absence of chemical bonds between chains. Accordingly, the crystal represents typical examples of one-dimensional magnetic lattice.

Belford et al. [14] investigated the pyrazine adduct, $Cu(hfac)_2$(paz) (hfac: $COCF_3CH_2CF_3CO$) of bis(1,1,1,5,5,5-hexafluoropentane-2,4-dionato)copper-(II), and confirmed the presence of —Cu—(paz)—Cu— chains analogous to those in $Cu(NO_3)_2$(paz). In Fig. 5, nitrate ions are replaced by (hfac) ions, and coordination octahedra are elongated along Cu—N directions. The Cu—N bond distance amounts to 2.529 Å indicating a rather weak bond. Belford et al. [14] report also that in the crystal of $[Cu(hfac)_2]_2$(paz), two molecules of $Cu(hfac)_2$ are bridged by a pyrazine molecule to form a binuclear cluster, in which each copper atom has a distorted square-pyramidal coordination elongated along the Cu—N bond (2.25 Å). Morosin et al. [15] found that the pyrazine adduct of copper(II) acetate has a structure characterized by alternating linear chains shown in Fig. 6, in which dimeric units of copper(II)

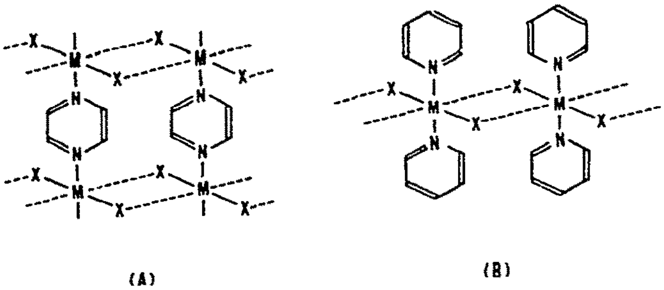

Fig. 4. Crystal structures of MX_2(pyrazine) (A) and MX_2(pyridine)$_2$ (B).

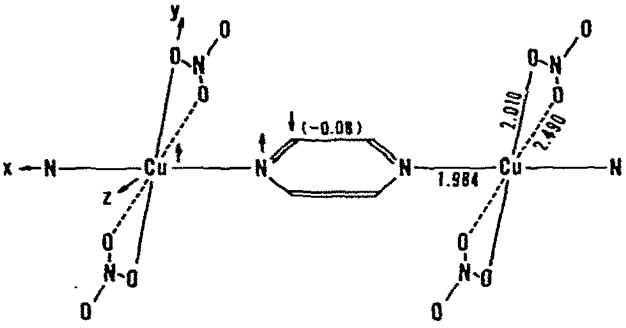

Fig. 5. Linear chain structure of $Cu(NO_3)_2(paz)$ and spin density on the ligand [13,62].

acetate monohydrate [16,17] are linked by pyrazine molecules. They performed X-ray crystal analysis at 300 and 100 K, and found that the Cu—Cu distance decreases from 2.583 to 2.576 Å with decreasing temperature.

Several bis(pyrazine) complexes, $CoX_2(paz)_2$ (X: Cl, Br, I), of cobalt(II) halides have been subjected to X-ray crystal analysis. Carreck et al. [18] found that in the crystal of $CoCl_2(paz)_2$, cobalt atoms are bridged by pyrazine molecules to form an infinite square array shown in Fig. 7 and that the resulting atomic sheets are stacked on one another by being shifted in parallel to themselves. The crystal forms a tetragonal lattice, the cell dimensions being a = 7.12 Å and c = 10.63 Å. $CoBr_2(paz)_2$, which is isomorphous with the foregoing compound, has lattice parameters, a = 7.16 Å and c = 11.2 Å [19]. It is interesting to note that the crystals of the two compounds have different cell dimensions along the c-axis but practically the same value along the a-axis that coincides with the direction of a —Co—(paz)—Co— chain.

Sletten [20] carried out X-ray analysis on the copper(II) complex of 6-aminopurine, $Cu(ap)_2 \cdot 4\ H_2O$, in which a condensed ring compound forms —M—L—M— links. Nitrogen atoms at positions 3 and 9 of 6-aminopurinate

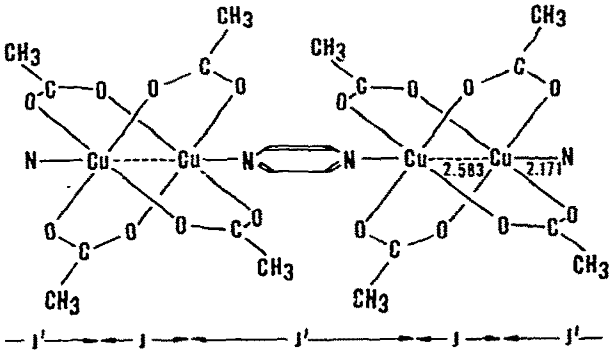

Fig. 6. Alternating linear chain of $Cu(CH_3COO)_2(paz)$ [15].

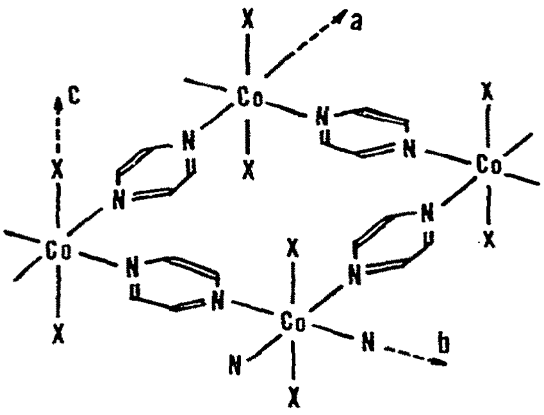

Fig. 7. Structure of $CoX_2(paz)_2$ (X: Cl, Br) [18].

ions are coordinated on two copper atoms to form a binuclear cluster bearing some resemblance to the dimeric cluster of copper(II) acetate monohydrate (see Fig. 8). The same type of dimeric structure has been found for $Cu(ClO_4)_2$-$(apH)_2 \cdot 2\ H_2O$ [21]. In this structure, nitrogen atoms at positions 3 and 9 of neutral 6-aminopurine molecules are coordinated on a pair of copper atoms to form $[Cu_2(apH)_4(H_2O)_2]^{4+}$. In a complex of copper(II) chloride with 6-

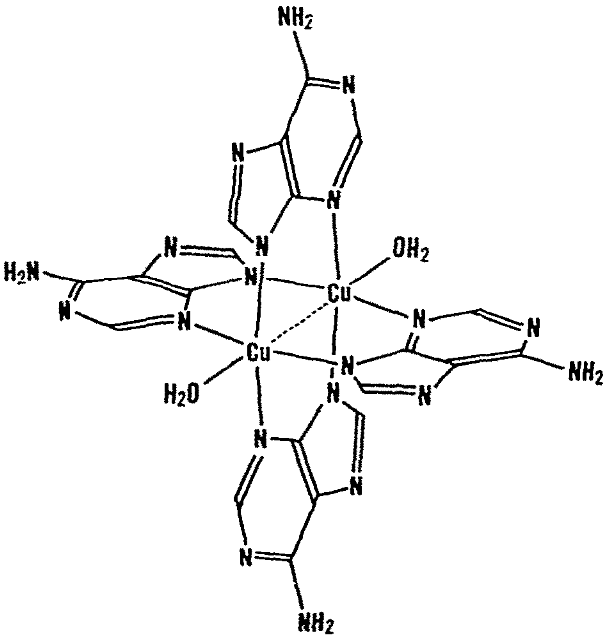

Fig. 8. Dimer structure of $Cu(ap)_2 \cdot 4\ H_2O$ [20].

aminopurine, $CuCl_2(apH)_2 \cdot 3\ H_2O$, and a similar complex with 6-hydroxypurine, $CuCl_2(hpH)_2 \cdot 3\ H_2O$, dimeric $[Cu_2L_4Cl_2]^{2+}$ ions exist as structural units [22—24]. The dimeric complex ion is of the same type as that in $Cu(ClO_4)_2(apH)_2 \cdot 2\ H_2O$ except that chloride ions rather than water molecules are involved in coordination. In the crystal of $[Cu_3Cl_8(apH_2)_2] \cdot 4\ H_2O$, neighboring copper atoms share two chloride ions and are bridged in addition by an $(apH_2)^+$ ion, thus forming linear trinuclear clusters [25]. In $CuBr_4(apH_2)_2$, two nitrogen atoms each at position 7 of a 6-aminopurinium ion are coordinated on a copper atom along with four bromide ions [26]. Accordingly, the structural unit is monomeric.

The X-ray crystal analysis of a nickel complex of 1,8-naphthyridine, $[Ni_2Br_2(1,8\text{-nph})_4] \cdot B(C_6H_5)_4$, in which nickel is apparently 1.5-valent, has revealed the existence of dimeric units bearing a close resemblance to those in $Cu(ap)_2 \cdot 4\ H_2O$ [27]. The dimeric unit is formed by four bridging Ni—N—C—N—Ni links each from a 1,8-naphthyridine molecule. The Ni—Ni distance in the dimer is as short as 2.415 Å.

C. A SURVEY ON THE THEORY OF SPIN INTERACTION

The Hamiltonian for the exchange interaction between electron spins S is given by

$$\mathcal{H} = -2 \sum_{i>j} J\mathbf{S}_i \cdot \mathbf{S}_j \tag{1}$$

where J stands for the exchange integral, a positive value of which implies ferromagnetic interaction while a negative value implies antiferromagnetic interaction. Although the summation should be taken over all conceivable combinations of $\mathbf{S}_i$ and $\mathbf{S}_j$, it is usually sufficient to take into account all pairs of nearest neighbors. The magnetic susceptibility of isolated clusters can be easily derived from eqn. (1) [28]. In the simplest case of binuclear clusters of spins equal to 1/2, the magnetic susceptibility is given by

$$\chi = \frac{N\mu_B^2 g^2}{3\,kT}\left[1 + \tfrac{1}{3}\exp\left(-\frac{2J}{kT}\right)\right]^{-1} + N\alpha \tag{2}$$

where N is the Avogadro number, μ_B denotes the Bohr magneton, g is the g-value, k is the Boltzmann constant, T is the absolute temperature, and $N\alpha$ denotes temperature-independent paramagnetism. For various types of clusters, the susceptibility has been formulated rigorously [28—33].

For a one-dimensional spin lattice, the Hamiltonian is given by

$$\mathcal{H} = -2J \sum_{i=1}^{N} [\mathbf{S}_{i,z} \cdot \mathbf{S}_{i+1,z} + \gamma(\mathbf{S}_{i,x} \cdot \mathbf{S}_{i+1,x} + \mathbf{S}_{i,y} \cdot \mathbf{S}_{i+1,y})] \tag{3}$$

where γ is a parameter expressing the extent of anisotropy of exchange interaction. The Ising model is based on extreme anisotropy ($\gamma = 0$), whereas the Heisenberg model refers to ideal isotropy ($\gamma = 1$). In the case of a linear Ising lattice of spins equal to 1/2, rigorous analytic formulae have been derived for parallel and perpendicular susceptibilities [34].

$$\chi_{\parallel} = \frac{N\mu_B^2 g_{\parallel}^2}{4\,kT} \exp\left(-\frac{J}{kT}\right) + N\alpha_{\parallel} \qquad (4)$$

$$\chi_{\perp} = \frac{N\mu_B^2 g_{\perp}^2}{4|J|}\left[\tanh\frac{|J|}{2\,kT} + \frac{|J|}{2\,kT}\operatorname{sech}^2\frac{|J|}{2\,kT}\right] + N\alpha_{\perp} \qquad (5)$$

The magnetic susceptibility of crystalline powder is given by

$$\chi = \tfrac{1}{3}(\chi_{\parallel} + 2\chi_{\perp}) \qquad (6)$$

No rigorous analytic formulae have been derived for a linear Heisenberg chain of S = 1/2. Bonner and Fisher [35] have performed numerical calculations for the susceptibility of N-membered rings (S_{N+1} is equivalent to S_1) with $N = 3$—11 in order to estimate the susceptibility of infinite chains by extrapolation. For linear Heisenberg chains of spins greater than 1/2, the susceptibility has not been calculated rigorously. However, the susceptibility formulated in the classical limit of infinite spins is applicable to lattices having a large spin quantum number [36]. The theoretical formula reproduces the temperature variation of the magnetic susceptibility of $CsMnCl_3 \cdot 2\,H_2O$, which contains —Mn—Cl—Mn— chains in crystals [37]. A rigorous theoretical calculation has been performed for the susceptibility of an alternating linear chain of S = 1/2 [38—41].

For two- and three-dimensional spin lattices, it is difficult to derive rigorous theoretical formulae even for S = 1/2, and several approximate formulae have been proposed [42]. In particular, the series expansion method gives a good approximation in the temperature range of $|J| << kT$ [43,44]. In this method, the reciprocal susceptibility is expressed by a power series of $|J|/kT$.

$$\frac{N\mu_B^2 g^2}{|J|\chi} = \frac{3}{S(S+1)}\left(\frac{kT}{|J|}\right)\sum_{n=0}^{\infty} b_n \left(\frac{|J|}{kT}\right)^n + N\alpha \qquad (7)$$

The values of b_n have been evaluated for various types of spin lattices. Ignoring terms having $n \geqslant 2$, one has the Curie—Weiss law

$$\chi = \frac{C}{T-\theta} + N\alpha \qquad (8)$$

in which C is the Curie constant, and θ is the Weiss constant, given by

$$\theta = \tfrac{2}{3} z S(S+1)\frac{J}{k} \qquad (9)$$

Here, z denotes the number of nearest neighbors.

Because strict analytic formulae are available for the susceptibility of various types of spin lattices of S = 1/2, exchange integrals can be evaluated for complexes containing metal atoms having a single unpaired electron. For this reason, copper complexes are particularly suitable as objects of magnetic studies. Often the dependence of magnetic susceptibility on temperature reveals the type of spin aggregation, which is closely related to crystal structure. It is thus possible to obtain structural information from magnetic data by taking into account the structures of analogous compounds already studied by X-ray analysis. In fact, a number of structures have been adequately proposed from observed magnetic susceptibility prior to the confirmation of the structures by X-ray crystal analysis.

When two metal ions are sufficiently close to each other as to lead to the overlap of orbitals of unpaired electrons, a metal—metal bond is formed through which direct spin interaction operates. When metal ions are bridged by a ligand, superexchange interaction takes place through it. The Cu—F—Cu system in potassium trifluorocuprate(II), $KCuF_3$, shown in Fig. 9 represents one of the simplest cases [45]. When the half-filled $d_{x^2-y^2}$ orbital of the Cu(1) atom overlaps the p_x orbital of a fluorine atom, partial transfer of an electron takes place from the latter orbital to the former. In this case, only an electron having its spin antiparallel to that in the $d_{x^2-y^2}$ orbital can take part in the transfer. In the p_x orbital, the fractional population of an electron having its spin parallel to the spin in Cu(1) predominates over that of antiparallel spin. Because the predominant spin induces an unpaired electron spin in the $d_{x^2-y^2}$ orbital of Cu(2), antiferromagnetic interaction operates between Cu(1) and Cu(2).

The sign and magnitude of exchange integrals depend on the symmetry and extension of orbitals involved in superexchange interaction as well as on the geometry of superexchange paths. It is difficult to calculate theoretically the accurate values of superexchange integrals, but the sign and the absolute values of J have been discussed to obtain rough estimations for various types of spin systems [46—48].

As is shown in Fig. 9, spin density is distributed on ligands, which otherwise are diamagnetic. If the spin density can be determined, valuable informa-

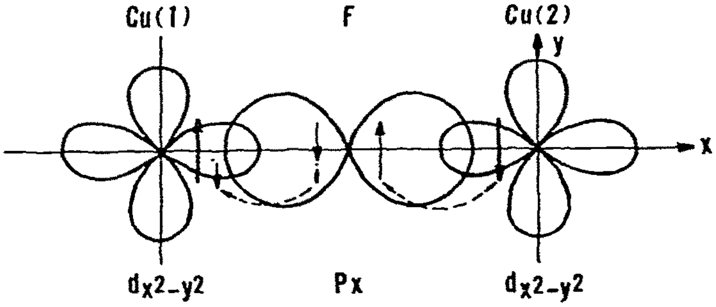

Fig. 9. Mechanism of superexchange interaction in Cu—F—Cu system.

tion can be obtained on the mechanism of the superexchange interaction. In fact, the superhyperfine structure of ESR absorptions and the Fermi contact shifts obtainable from NMR can afford information about spin delocalization on ligands in metal complexes. In particular, the Fermi contact shift method has an advantage that the sign of the spin density can be determined. The high-resolution PMR of various metal complexes in solutions has indicated spin delocalization in ligands, and has given valuable information about the nature of metal—ligand bonds [49,50]. In order to elucidate the mechanism of superexchange interaction, one must observe PMR in the crystalline state. However, the PMR spectra of solids are in general broad. Hence determination of contact shifts usually involves some difficulties for complexes having various kinds of non-equivalent protons in ligands because it is difficult, in such cases, to resolve the absorption curve into component curves attributable to one kind of equivalent protons. Fortunately, the metal complexes of diazoles and diazines are amenable to the NMR method because only a few kinds of non-equivalent protons are contained in these complexes. The Fermi contact shift is given by [49—52]

$$\frac{\Delta H}{H} = -a\,\frac{\chi - N\alpha}{g_{\mathrm{N}}\mu_{\mathrm{N}}N} \tag{10}$$

Here $\Delta H/H$ denotes the Fermi contact shift, a is a coupling constant (in Oe), and g_{N} and μ_{N} are the g-factors of the nucleus and the nuclear magneton, respectively. The coupling constant a is related to the spin density ρ on a carbon or nitrogen atom bonded to the resonant proton by [51,53]

$$a = Q\rho \tag{11}$$

where Q is a proportionality constant characteristic of the particular mechanism giving rise to interaction between a nuclear spin and an electron spin. The absolute values of Q have been determined by ESR experiments on a variety of free radicals. The sign of Q and ρ are not determinable from the ESR experiments. However, the signs of ρ in paramagnetic systems are manifested in NMR experiments by the direction of resonance field shifts because the sign of Q is determined theoretically. For aromatic · C—H fragments, Q has been empirically determined as $Q(\mathrm{CH}) = -22.5$ Oe as an average value [54]. On the other hand, few data are available in the literature on the values of $Q(\mathrm{NH})$ for protons bonded to a nitrogen atom involved in a a heterocyclic ring. Barton and Fraenkel [55] have carried out ESR experiments on pyrazine cation radicals. By use of $Q(\mathrm{CH}) = -23.7$ Oe, they obtained $Q(\mathrm{NH}) = -33.7$ Oe for protons attached to nitrogen. Because the sign and the approximate values of Q are already known, one can find the sign as well as the absolute value of ρ. A positive value of ρ implies the presence of spin density in parallel to the unpaired electron spin on a central metal, and vice versa.

D. COMPLEXES OF PYRIDAZINE AND ITS ANALOGS

Exobidentate pyridazine can form —M—N—N—M— links. Accordingly, it is expected that linear chains of the same type as in $CuCl_2(trH)$ are formed in the crystals of $CuX_2(pid)$ type complexes (X: Cl, Br). Emori et al. [56] determined the magnetic susceptibilities of $CuX_2(pid)$ and $CuX_2(pht)$ in a temperature range of 4.2—300 K.

The magnetic susceptibility of $CuCl_2(pid)$ plotted against the temperature shows a broad maximum at about 60 K attributable to interaction within one-dimensional chains as shown in Fig. 10. Below 20 K, the susceptibility increases sharply with decreasing temperature. This behavior is due either to a trace of magnetically isolated metal ions or to magnetic interaction between one-dimensional lattices. The contribution of this effect to susceptibility is assumed to be given by the second term in the following equation in accordance with the Curie law, C_{low} being the Curie constant for the susceptibility in the low temperature range.

$$\chi = \chi_{\mathrm{linear}} + C_{\mathrm{low}}/T \tag{14}$$

where χ_{linear} is the susceptibility intrinsic in one-dimensional lattices given by

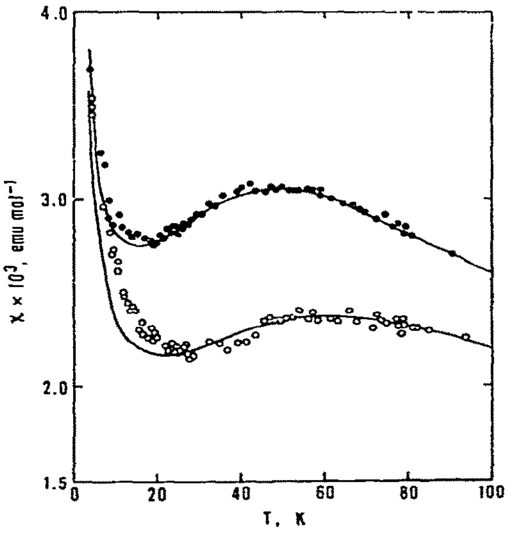

Fig. 10. Magnetic susceptibilities of $CuCl_2(pid)$ (○) and $CuCl_2(pht)$ (●) and theoretical curves based on the linear Heisenberg model [56].

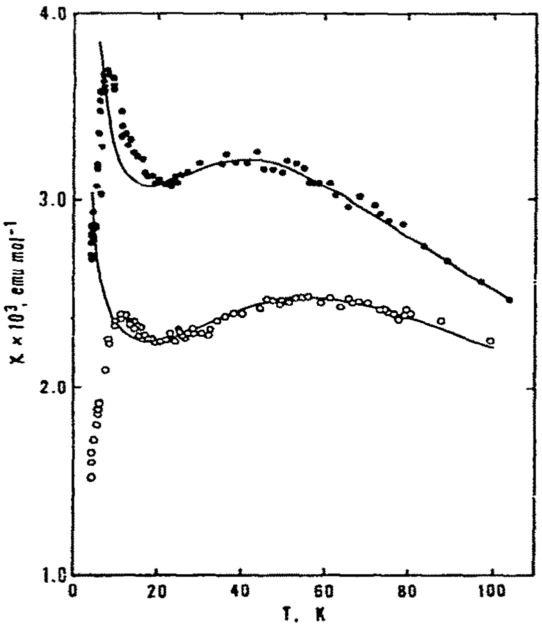

Fig. 11. Magnetic susceptibilities of $CuBr_2(pid)$ (○) and $CuBr_2(pht)$ (●) and theoretical curves based on the linear Heisenberg model [56].

eqns. (4) and (5) for the Ising model and by Bonner—Fisher's theoretical curve for the Heisenberg model. Above about 200 K, the susceptibility obeys the Curie—Weiss law. Denoting the Curie constant by C_{high}, one can estimate the fractional concentration of copper ions participating in the paramagnetic behavior in the low temperature range by $C_{\mathrm{low}}/C_{\mathrm{high}}$. The ratio is equal to 0.0003, indicating that only a trace of isolated metal ion is involved in the low temperature paramagnetism. The observed temperature dependence of susceptibility can be well reproduced by a full curve in Fig. 10 if Bonner—Fisher's theoretical curve is used for χ_{linear}. The values of parameters, J and g, are listed in Table 1. Hyde et al. [57] evaluated the zero-field splitting constant from the line width of ESR as about 5×10^{-2} cm^{-1}, and estimated the anisotropy parameter γ to be almost equal to unity. Accordingly, the Heisenberg model is more adequate in this case than the Ising model. In fact, formulae (4)—(6) for the Ising model do not reproduce observed susceptibility unless an abnormally small value is chosen for the g-value.

The susceptibility of $CuBr_2$(pid) shows two maxima at about 12 and 55 K, as shown in Fig. 11 [56]. The maximum on the high temperature side is due to interaction within chains, whereas that on the low temperature side is attributable to interaction between chains. The susceptibility in the high temperature region was analyzed by the same method as used for $CuCl_2$(pid) and gave results shown in Table 1. The g-value is smaller than the value of $g \sim 2.1$ commonly observed for a variety of copper(II) complexes and also smaller than the g-value (2.13) evaluated from the Curie constant in the high temperature region. Presumably, interaction between chains is so strong that models based on isolated chains are no longer adequate. The appearance of the low temperature maximum supports this view.

The temperature dependence of the susceptibilities of CuX_2(pht) (X: Cl,

TABLE 1

Magnetic parameters of CuX_2(pid) and related compounds: Weiss and Curie constants, θ_{high} and C_{high}, at high temperatures, g-value g_C evaluated from C_{high}, and parameters, J, g, and C_{low}, evaluated by assuming the linear Heisenberg model [56,96]

Compound	θ_{high} (K)	C_{high}	g_C	J/k (K)	g	C_{low}
$CuCl_2$(pid)	−61.5	0.413	2.10	−51.7	2.06	0.000135
$CuBr_2$(pid)	−69.0	0.424	2.13	−45.8	1.98	0.000129
$CuCl_2$(pht)	−61.2	0.440	2.17	−40.6	2.08	0.000151
$CuBr_2$(pht)	−47.4	0.404	2.08	−36.0	1.98	0.000274
$CuCl_2$(trH) [a]	−19.0	0.426	2.13	−17.9	2.07	0.027
$CuBr_2$(trH) [a]	−6.7	0.424	2.13	−8.3	2.10	0.046
$CuCl_2$(atrH)	−18.3	0.427	2.13	−17.6	2.17	0.000377
$CuBr_2$(atrH)	−10.1	0.413	2.10	−7.58	1.93	— [b]

[a] The parameters were evaluated on the basis of the linear Ising model.

[b] No paramagnetic behavior was observed at low temperature.

Br) bears a striking resemblance to that of the corresponding pyridazine complexes as shown in Figs. 10 and 11. The exchange integral of CuX_2L (X: Cl, Br; L: pid, pht) varies with the kind of ligands but not so much with the kind of halogens, indicating that superexchange interaction takes place mainly through the heterocycles.

Tetradentate bridging ligands can be prepared by introducing some groups capable of being coordinated into pyridazine or phthalazine. Andrew et al. [58] synthesized nickel(II) and cobalt(II) complexes I—III, and observed the temperature dependence of susceptibility in a temperature range of 80—300 K. Lever et al. [59] determined the susceptibility of a cobalt(II) complex IV over 80—300 K. Since these complexes are suspected to form binuclear clusters, susceptibility has been analyzed by theoretical formulae for binuclear clusters consisting of spins S = 3/2 or 1. Although no susceptibility maxima were observed in the temperature range of observation, the values of J were deter-

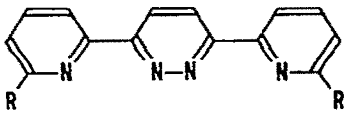

(I) R : H, dpp
(II) R : CH_3, mdpp

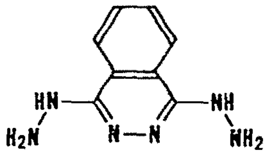

(III) dhp

TABLE 2

Magnetic parameters of some binuclear cobalt(II) and nickel(II) complexes [58,59]

Compound	M = Co		M = Ni		J_{Ni}/J_{Co}
	$-J/k$ (K)	g	$-J/k$ (K)	g	
$M(NO_3)_2(dpp) \cdot H_2O$	10.6	2.38	33.8	2.22	3.2
$M(ClO_4)_2(dpp) \cdot n\ H_2O$ [a]	8.2	2.26	21.1	2.15	2.6
$M_2(SO_4)_2(dpp) \cdot 5\ H_2O$	7.5	2.41	17.7	2.18	2.4
$M_2(NO_3)_4(mdpp)$ [b]	11.6	2.41	29.8	2.18	2.6
$MCl_2(dhp) \cdot n\ H_2O$ [a]	10.6	2.39	32.1	2.15	3.0
$MBr_2(dhp) \cdot 3\ H_2O$	11.9	2.41	34.3	2.16	2.9
$M_2Cl_3(dap)$	4.88 [c]	2.24_7	—	—	
$M_2Br_3(dap)$	6.23 [c]	2.17_8	—	—	
$M_2I_3(dap)$	7.90 [c]	2.15_0	—	—	

[a] The number n of water of hydration is different between the cobalt(II) and nickel(II) complexes.
[b] M = Co, methanol adduct; M = Ni, hydrate.
[c] The values are reported in cm^{-1} in ref. 59.
Abbreviations: dpp, 3,6-di(2-pyridyl)pyridazine; mdpp, 3,6-di(6-methyl-2-pyridyl)pyridazine; dhp, 1,4-dihydrazinophthalazine; dapH, 1,4-di(2-pyridyl)aminophthalazine.

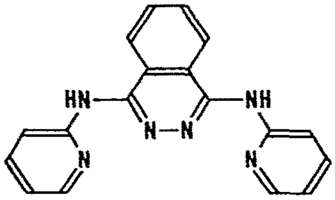

(IV) dapH

mined as shown in Table 2. The absolute values of J of nickel(II) complexes are 2—3 times as large as those of the corresponding cobalt(II) complexes. Andrew et al. [58] presume that coupling between t_{2g} electrons contributes to ferromagnetic interaction in cobalt(II) complexes.

E. COMPLEXES OF PYRIMIDINE

The magnetic susceptibility of $CuCl_2$(pim) has been determined from 110 to 369 K [57]. It changes monotonically with temperature. Although the crystal structure of this compound has not as yet been clarified, the susceptibility has been analyzed by assuming eqn. (4), and yielded a J-value equal to $-39\ cm^{-1}$ or $J/k = -56$ K. Because the exchange integral is comparable with that of $CuCl_2$(pid), it is undoubtable that —Cu—(pim)—Cu— links are formed in crystals.

F. COMPLEXES OF PYRAZINE AND ITS ANALOGS

Because $Cu(NO_3)_2$(paz) has a structure as shown in Fig. 5, it is expected to show magnetic properties characteristic of one-dimensional lattices. By applying magnetic field in parallel and at right angles to —Cu—(paz)—Cu— chains, Losee et al. [60] determined magnetic susceptibilities, $\chi_\parallel$ and $\chi_\perp$, in a temperature range of 1.7—60 K, as shown in Fig. 12. Broken curves were calculated by eqns. (4) and (5) for the Ising model, according to which $\chi_\parallel$ vanishes while $\chi_\perp$ assumes a finite value at absolute zero temperature. Observed susceptibilities show no sign of this type of anisotropy. On the other hand, Bonner—Fisher's theoretical curves based on the linear Heisenberg model reproduce well the observed susceptibilities, and yield $J/k = -5.30$ K in both parallel and perpendicular directions and $g_\parallel = 2.03$ and $g_\perp = 2.10$ for g-values. The single-crystal ESR spectrum of the complex yielded three g-factors, $g_x = 2.0563$, $g_y = 2.0742$, and $g_z = 2.2740$, the axes of which are defined in Fig. 5 [61]. The parallel and perpendicular g-values determined from the magnetic susceptibility agree well with the values, $g_\parallel = g_x = 2.0563$ and $g_\perp = [\frac{1}{2}(g_y^2 + g_z^2)]^{1/2} = 2.1763$, evaluated from the data of the ESR experiment. This supports the validity of the linear Heisenberg model.

Inoue et al. [62] recorded the broad-line PMR spectrum of crystalline powder of $Cu(NO_3)_2$(paz). The composite derivative curve showing a low-field shift can be decomposed into two simple derivative curves as is done in Fig. 13.

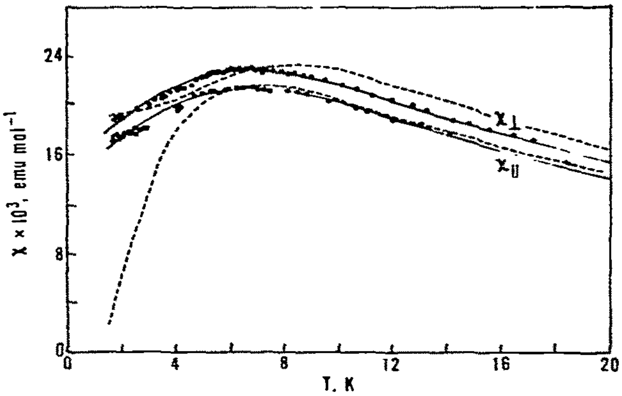

Fig. 12. Magnetic susceptibility of the single crystal of $Cu(NO_3)_2(paz)$ and theoretical curves based on the linear Heisenberg model (solid curves) and the linear Ising model (broken curves) [60].

Equation (10) indicates that the contact shift is directly proportional to resonance field strength and bulk magnetic susceptibility corrected for the temperature-independent paramagnetism. In the temperature range of the PMR experiment, the magnetic susceptibility obeys the Curie—Weiss law with a Weiss constant of —6 K. The observed shift ΔH varies with temperature obey-

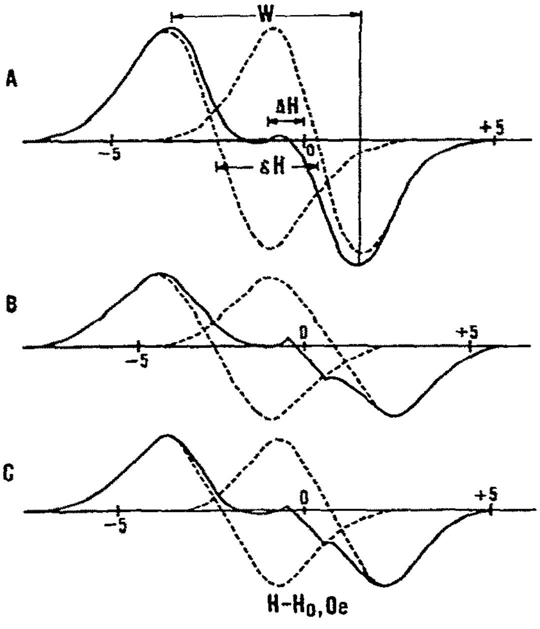

Fig. 13. Broad-line PMR absorption derivative curves observed at 30 MHz and room temperature. A, $Cu(NO_3)_2(paz)$; B, $CuCl_2(paz)$; C, $CuBr_2(paz)$ [62].

ing the Curie—Weiss law (see Table 3 and Fig. 14), whereas the separation δH between the centers of the component curves is almost independent of temperature, because the peak-to-peak width W shows no marked variation with temperature. The shift ΔH was confirmed to depend on the magnetic field strength as well. These facts indicate that ΔH is due to the contact shift and that the origin of the composite curve is the dipole interaction between protons in a pyrazine molecule. In Fig. 13, δH can be approximated to $3\mu/r^3$ where r denotes the distance between neighboring protons. From $\delta H = 2.6$ Oe, r is calculated to be equal to 2.5 Å in agreement with 2.3 Å as determined by X-ray crystal analysis. From the observed susceptibility and ΔH, the coupling constant a was calculated (Table 3), and the spin density on carbon atoms adjacent to nitrogen was evaluated by eqn. (11) as $\rho_C = -0.08$ using $Q(\mathrm{CH}) = -23.7$ Oe.

The $p\pi$ orbitals of the carbon atoms are populated by unpaired electrons having their spins antiparallel to that in the $d_{x^2-y^2}$ orbital of a copper(II) ion (see Fig. 5). The distribution of the negative spin density is presumed to take place in accordance with the following mechanism. In the first place, a positive spin density in the $p\pi$ orbital of a nitrogen atom due to the polarization of a metal—ligand σ bond induces a negative spin density in the $p\pi$ orbitals of adjacent carbon atoms by polarizing the N—C π bonds. Secondly, one must take into account the diffusion through a Cu—N π bond of unpaired electrons raised into the t_2 orbitals of copper owing to the mixing of the e and t_2 orbitals due to spin—orbit coupling.

Inoue et al. [62] observed the magnetic susceptibility and broad-line PMR of $CuX_2(paz)$ (X: Cl, Br). As shown in Fig. 15, the susceptibility can be reproduced by Bonner—Fisher's theoretical curves very well, and yields J-values given in Table 4. It is known that bis(pyridine) complexes, $CuX_2(pyridine)_2$ (X: Cl, Br), assume a structure shown in Fig. 4(B), in which

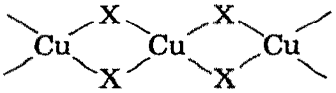

TABLE 3

Contact shift $\Delta H/H_0$, peak-to-peak width W, coupling constant a, spin density ρ on a carbon atom, and magnetic parameters J, g of $CuX_2(paz)$ [62]

Compound	$\Delta H/H_0 \times 10^4$ (T, K)	W (Oe) (T, K)	a (Oe)	ρ	J/k (K)	g
$Cu(NO_3)_2(paz)$	−1.4 (295)	4.8 (295)	1.9	−0.08	−5.2	2.07
	−2.7 (156)	5.8 (156)				
$CuCl_2(paz)$	−1.4 (293)	7.0 (293)	1.8	−0.08	−14.6	2.03
	−1.9 (198)	7.6 (198)				
$CuBr_2(paz)$	−1.2 (298)	6.2 (298)	1.6	−0.07	−24.2	2.03
	−1.6 (197)	6.4 (197)				

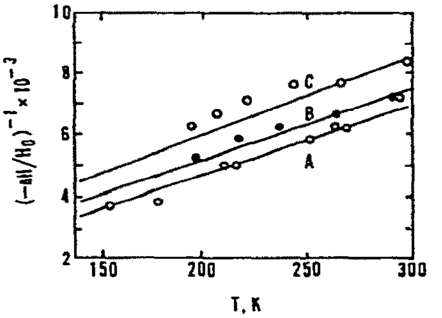

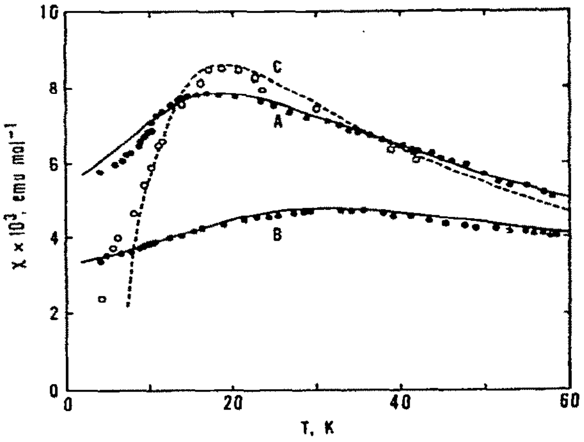

Fig. 14. The reciprocal of shifts $\Delta H/H_0$ is plotted against the temperature. The solid curves represent the theoretical shifts calculated by eqn. (10) with the coupling constants listed in Table 3 and the susceptibilities evaluated from the Curie and Weiss constants. A, $Cu(NO_3)_2(paz)$; B, $CuCl_2(paz)$; C, $CuBr_2(paz)$ [62].

Fig. 15. Magnetic susceptibilities of $CuCl_2(paz)$, A; $CuBr_2(paz)$, B; and $CuCl_2(2\text{-}mpaz)$, C. The solid curves are based on the linear Heisenberg model, while the broken curve is based on the dimer model [62,69].

chains are not crosslinked. The J-values of $CuX_2(paz)$, $J/k = -14.6$ and -24.2 K, respectively, are close to those of the corresponding values of the bis(pyridine) complexes, $J = -9.15$ cm^{-1} or $J/k = -13.2$ K for the chloride complex and $J = -18.9$ cm^{-1} or $J/k = -27.2$ K for the bromide complex [63,64]. The broad-line PMR spectra of $CuX_2(paz)$ bear a close resemblance to that of Cu-

TABLE 4

Magnetic parameters, J and g, and π—π^* transition of $Cu(NO_3)_2(L)$ and pK_1 of the ligands [66,67]

Ligand	$-J$ (cm^{-1})	g	π—π^* (10^3 cm^{-1})	pK_1[a]
Phenazine	6.3	2.14	27.6	1.23
Quinoxaline	4.5	2.14	29.0	0.56
2,6-Dimethylpyrazine	4.0	2.10	35.1	1.90
Pyrazine	3.7	2.08	34.6	0.65
2,5-Dimethylpyrazine	3.5	2.10	33.7	1.85
Methylpyrazine	3.1	2.06	34.2	1.45
Chloropyrazine	1.4	2.09	36.4	—
1,5-Naphthyridine	10.8	2.10	—	—
1,4,5-Triazanaphthalene	9.6	2.07	—	—

[a] The pK of dissociation of monoprotonated bases.

$(NO_3)_2$(paz) (see Fig. 13); the spin density on carbon atoms is almost the same in the three complexes, indicating that superexchange interaction operates to almost the same extent through —Cu—(paz)—Cu— paths. The fact that nevertheless the J-value depends to a great extent on the kind of anionic components leads to the conclusion that the mechanism of spin interaction is governed by —Cu—X—Cu— links rather than the —Cu—(paz)—Cu— paths in the halide complexes.

The magnetic susceptibilities of $Cu(NO_3)_2L$ type complexes having pyrazine analogs as the ligand can also be explained by Bonner—Fisher's curves. Accordingly, it is concluded that one-dimensional chains are formed [65—67].

Richardson and Hatfield [67] determined the J-values of a series of compounds listed in Table 4, and also recorded their electronic spectra. They observed an absorption at 27,000—36,000 cm^{-1} in addition to a d—d band appearing at about 18,000 cm^{-1}. They assigned the former to the π—π^* transition of ligands, and pointed out a close relation between the transition energy and the J-value. On the other hand, the J-value shows no relation to the pK_1 value (pK of the dissociation of monoprotonated bases), which expresses the donor capacity of σ-electrons in nitrogen atoms. From these facts, the authors propose a mechanism in which unpaired electrons in the $d_{x^2-y^2}$ orbital diffuse into ligand molecules through the direct overlap of the d-orbital of copper with the $p\pi$ orbital of carbon atoms.

Stoklosa et al. [66] found that the magnetic susceptibility of $Cu(NO_3)_2L$ type complexes having 1,5-naphthyridine (1,5-nph) and 1,4,5-triazanaphthalene (taz) as ligands could be expressed by Bonner—Fisher's theoretical formula for linear chains. They concluded that one-dimensional —Cu—(1,5-nph)—Cu— chains are formed and that nitrogen atoms at positions 1 and 5 of the nitrogen heterocycle (see Fig. 1) must be coordinated on two different copper atoms. The same type of one-dimensional chains, —Cu—(taz)—Cu—, are suspected for the 1,4,5-triazanaphthalene complex as well. The absolute values of J of the two compounds are much greater than those of the corresponding pyrazine and phenazine complexes as shown in Table 4.

The copper halide complexes of 2,6-dimethylpyrazine and 2,5-dimethylpyrazine, CuX_2L, have been suspected to have a structure shown in Fig. 4(A), and the magnetic susceptibility has been analyzed by the linear Ising model [68,69]. On the other hand, the magnetic susceptibility of 2-methylpyrazine complexes, CuX_2(2-mpaz) (X: Cl, Br) show a temperature dependence quite different from that of CuX_2(paz) [69]. In Fig. 15, the susceptibility of the chloride complex is plotted against the temperature. Curve C was calculated for the chloride complex by eqn. (2) using $g = 1.89$ and $J = -10.5$ cm^{-1} ($J/k = -15.1$ K). The dimer model seems to be more suitable than the one-dimensional chain model although the g-value must be assumed to be abnormally small. It is presumed that owing to the low symmetry of the ligand, the lattice shown in Fig. 4(A) is distorted to give rise to pairing of copper atoms.

The CuX_2L_2 type complexes of pyrazine derivatives also show magnetic susceptibility characteristic of one-dimensional magnetic lattices, and the structure shown in Fig. 4(B) is anticipated [69,70]. For the CuX_2L and CuX_2L_2 (X: Cl, Br, NO_3) type complexes of quinoxaline and its derivatives, effective magnetic moments have been determined only at room temperature [71—73].

The pyrazine complex of copper(II) acetate, $Cu(CH_3COO)_2(paz)$, presumably represents an alternating linear antiferromagnet as shown in Fig. 6. Because exchange integrals differ from each other very much, i.e., $|J| >> |J'|$, only J has been determined from the temperature dependence of magnetic susceptibility as $J/k = -230$ K, whereas J' has been estimated to be equal to about 1100 Oe (~ 1 cm^{-1}) from the line width of ESR [15,74].

The magnetic susceptibility of $CoX_2(paz)_2$ (X: Cl, Br) having a structure shown in Fig. 7 has been determined in a temperature range of 1.8—300 K. However, no marked behavior revealing the presence of exchange interaction has been found [19]. The susceptibility of $NiX_2(paz)_2$ (X: Cl, Br, I) has been observed from 90 to 300 K. The Weiss constant amounts to only +2 to +4 K, indicating a very weak interaction [75].

The magnetic susceptibility of $AgS_2O_8(paz)_2$ obeys the Curie—Weiss law from 80 to 300 K; the Weiss constant equal to −84 K is very large in its absolute value [76]. The effective magnetic moment is equal to 1.61 B.M. at 299 K and decreases to 1.27 B.M. at 83 K. A network structure involving —Ag—(paz)—Ag— links has been proposed. The large negative Weiss constant of the silver complex is noteworthy in contrast with very weak spin interaction through pyrazine in the copper(II), nickel(II), and cobalt(II) complexes.

The magnetic moments of a variety of complexes presumably having pyrazine bridging have been determined at room temperature, but none of them reveals definitely the presence of spin interaction [77—80].

Reports have been published on the magnetic susceptibilities of copper(II) complexes having pyrazine derivatives as tetra- or hexadentate ligands [76,81]. Pyrazine-2,3-dicarboxylatocopper(II) is suspected to have a linear chain structure V. From its magnetic susceptibility determined in a temperature range of 80—300 K, the Weiss constant was evaluated as −4 K [76]. Fleischer et al. [81] synthesized a copper(II) complex VI, and confirmed the existence of a

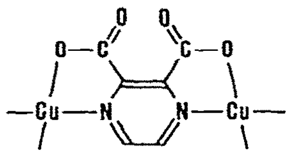
(V)

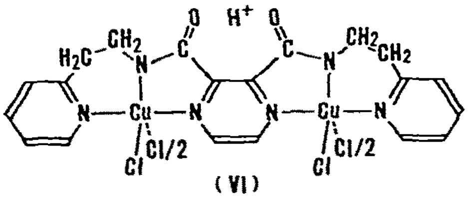
(VI)

dimer structure by X-ray crystal analysis. They observed the magnetic susceptibility down to 4.8 K, and found that it deviates from the Curie—Weiss law below about 12 K, the Weiss constant being equal to —1.5 K.

G. COMPLEXES OF PYRAZOLE

The uninegative anion of pyrazole acts as a bridging ligand. A number of metal complexes of this type have been synthesized, and the existence of dimeric or polymeric structures has been concluded [82—87]. The temperature variation of the susceptibility of $Cu(py)_2 \cdot 1/2\ H_2O \cdot 1/2\ NH_3$ has been determined in a temperature range of 80—300 K [87]. It shows a broad maximum at about 130 K, and can be expressed by a Bonner—Fisher's theoretical curve for a one-dimensional lattice with $J/k = -105$ K and $g = 2.08$. A copper(II) complex having a pyrazolate ion at position X in VII has been synthesized. Its susceptibility can be explained by eqn. (2) for dimeric clusters over a temperature range of 80—300 K, the exchange integral being determined as —160 to —186 cm^{-1} or $J/k = -230$ to -259 K [84,86]. Probably, a pyrazolate ion is coordinated on a pair of copper atoms with two nitrogen atoms to form a Cu—N—N—Cu link. However, the possibility of bridging through a single nitrogen atom cannot be entirely ruled out [86].

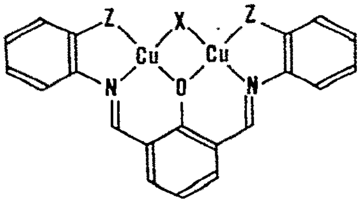

(VII) Z:O,S

H. COMPLEXES OF IMIDAZOLE

A large number of the metal complexes of imidazole have been synthesized, and their structures have been discussed. Some have been subjected to X-ray analysis, while others are conceived to have imidazole bridges from consideration of chemical composition [83,88—94]. $CuCl(im)(imH)_2$ has been subjected to X-ray crystal analysis and magnetic investigation at room temperature [93]. The effective magnetic moment was found to be equal to 1.68 B.M., whereas those of the corresponding bromide and iodide complexes are equal to 1.69 and 1.71 B.M., respectively [93], suggesting the presence of spin interaction through imidazolate ions. Three magnetically different modifications have been reported for $Cu(im)_2$ [83]: a brown modification (effective magnetic moment, 1.46 B.M. at room temperature), a blue modification (1.57 B.M.), and a green modification (1.62 B.M.). Jarvis and Wells [3] do not describe the method of synthesis of their sample employed for X-ray crystal analysis, but they seem to have used the blue modification. Inoue and Kubo [87] determined the magnetic susceptibility of the three modifications in a temperature range of 80—300 K. The susceptibility of the blue modification obeys the Curie—Weiss law in the whole range of temperature investigated, the Weiss constant being equal to —156 K. The green modification obeys the law below 170 K, yielding θ equal to —101 K. The brown modification shows a broad maximum of susceptibility at about 110 K. In all of these modifications, a strong antiferromagnetic interaction operates through —Cu—(im)—Cu— links.

The complexes of various metalloporphyrins with imidazole have been studied owing to their biological importance. Cohen and Ostfeld [95] synthesized the iron(III) tetraphenylporphin ($tppH_2$) complex of imidazole, Fe(tpp)(im) · H_2O, and determined its magnetic susceptibility in the temperature range of 4.2—300 K. The susceptibility assumes its maximum at 80 K and increases sharply with decreasing temperature below 40 K. The field dependence of the susceptibility was examined in a temperature range of 77—300 K under a field strength H of 0—13 kOe. From a plot of χ vs. $1/H$, the authors found that the susceptibility consists of a component independent of the magnetic field strength and another component dependent on the field. The former yields an effective magnetic moment equal to 2.15 B.M. at 300 K and 1.9—2.1 B.M. at 77 K. The latter component amounts to about 22×10^{-3} emu mol^{-1} at 300 K and decreases to 4×10^{-3} emu mol^{-1} at 80 K under a field strength of 6.44 kOe. The authors insist that the behavior is intrinsic in —Fe—(im)—Fe— chains, and is not due to impurities.

I. COMPLEXES OF 1,2,4-TRIAZOLE

Dichloro(1,2,4-triazole)copper(II), $CuCl_2(trH)$, has a structure in which two neighboring nitrogen atoms in a molecule of the nitrogen heterocycle are coordinated on two copper atoms bridged in addition by two chlorine atoms, copper atoms being arranged in a one-dimensional array as shown in Fig. 2 [1]. Its magnetic susceptibility shows a maximum at about 11 K and a minimum at about 8 K, below which it increases with decreasing temperature in accordance with the Curie—Weiss law [96]. The χ—T curve resembles that of $CuCl_2(pid)$ qualitatively. The magnetic susceptibility of $CuBr_2(trH)$ [56] increases at high temperature with decreasing temperature by obeying the Curie—Weiss law. Below 40 K, it deviates from the law without showing any clear maximum. With decreasing temperature below 6 K, it increases sharply in accordance with the Curie—Weiss law. The susceptibilities of these compounds have been analyzed tentatively by eqn. (4) for the parallel susceptibility of the linear Ising model, and have yielded exchange integrals shown in Table 1. Unlike in other halide complexes, the interaction is weaker in the bromide complex than in the corresponding chloride.

The PMR derivative curve of $CuCl_2(trH)$ [56,97] is asymmetric and can be decomposed into two simple derivative curves of intensity ratio equal to 2 : 1

as shown in Fig. 16. Since all 1,2,4-triazole molecules are equivalent in a crystal, the two component curves are attributable to two kinds of non-equivalent protons in a 1,2,4-triazole molecule. From the intensity ratio, the component curve showing a low-field shift is assigned to CH protons, whereas that of a high-field shift is attributed to NH protons. From the observed shifts $\Delta H/H$, the spin densities are calculated by eqns. (10) and (11) using $Q(\mathrm{CH}) = -23.7$ Oe and $Q(\mathrm{NH}) = -33.7$ Oe as $\rho_C = -0.08$ and $\rho_N = +0.06$. The PMR derivative curve of $CuBr_2(trH)$ is essentially the same as that of the foregoing compound, and yields $\rho_C = -0.11$ and $\rho_N = +0.08$. The spin densities are practically indistinguishable from those of the chloride complex because the decomposition of composite derivative curves involves uncertainty to some extent. It is a characteristic of π spin delocalization that positive and negative spin densities are distributed alternately, and that the absolute value of density shows no particular tendency towards its attenuation [50]. Spin delocalization in the complexes is induced through π spin delocalization, and a positive spin density is distributed on each nitrogen atom adjacent to a copper atom. The presence of spin density on the π system of the ligand indicates the adequacy of superexchange interaction through the nitrogen heterocycles.

Although $CuSO_4(trH)_2 \cdot 3\ H_2O$, $CuCl(tr) \cdot 2\ H_2O$, and $Cu(tr)_2$ have not as yet been subjected to X-ray crystal analysis, the temperature dependence of magnetic susceptibility observed in a range of 80—300 K indicates plausible types of spin aggregation [87]. The susceptibility of $CuSO_4(trH)_2 \cdot 3\ H_2O$ shows a broad maximum at about 100 K and can be explained by the linear Heisenberg model with $J/k = -80$ K and $g = 2.09$. $CuCl(tr) \cdot 2\ H_2O$ has an effective magnetic moment of 1.32 B.M. at room temperature. Its susceptibility increases with decreasing temperature without obeying the Curie—Weiss law. This behavior is characteristic of magnetic clusters containing an odd number of copper atoms; a trinuclear cluster is considered to be the most probable structural unit ($J/k = -155$ K). The magnetic susceptibility of $Cu(tr)_2$ obeys the Curie—Weiss law ($\theta = -87$ K) in the whole temperature range investigated, suggesting a network structure as in $Cu(im)_2$.

The copper(II) complex of 4-amino-1,2,4-triazole, $CuCl_2(atrH)$, shows a susceptibility vs. temperature curve resembling that of $CuCl_2(pid)$ [56]. On

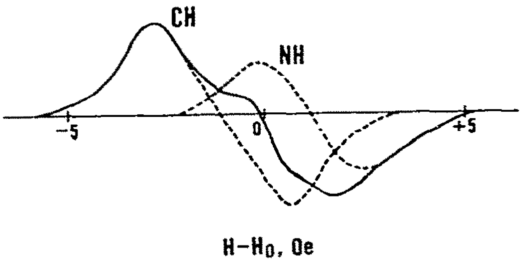

Fig. 16. PMR of crystalline powder of $CuCl_2(trH)$ [97].

the other hand, the susceptibility of $CuBr_2(atrH)$ can be reproduced neither by the linear Heisenberg model nor by the linear Ising model unless an abnormally small value is assumed for the *g*-value (Table 1), indicating the presence of a strong interaction between chains.

J. COMPLEXES OF CONDENSED RING HETEROCYCLES

The copper(II) complexes of 6-aminopurine and 6-hydroxypurine such as $Cu(ap)_2 \cdot 4\ H_2O$, $CuCl_2(apH)_2 \cdot 3\ H_2O$, and $CuCl_2(hpH)_2 \cdot 3\ H_2O$ having a dimer structure shown in Fig. 8 gradually lose their water of crystallization in air. Accordingly, the determination of magnetic susceptibility involves some difficulties. In fact, the exchange integral of $Cu(ap)_2 \cdot 4\ H_2O$ evaluated by eqn. (2) shows the scatter of data over -105 to $-129\ cm^{-1}$ ($J/k = -151$ to -186 K) [98,99]. When dried over silica gel, these compounds yield $Cu(ap)_2 \cdot 3\ H_2O$, $CuCl_2(apH)_2 \cdot 3/2\ H_2O$, and $CuCl_2(hpH)_2 \cdot H_2O$, respectively, which no longer lose their water of crystallization even in a vacuum. The susceptibility of each of these compounds can be expressed by eqn. (2) for binuclear clusters, yielding exchange integrals shown in Table 5 [100]. The corresponding bromide complexes also show a similar variation of susceptibility with temperature. Some mono(6-aminopurine)copper(II) complexes also show χ—T curves characteristic of binuclear clusters, the *g*- and *J*-values being listed in Table 5 [100].

TABLE 5

Magnetic parameters of some copper(II) complexes having binuclear structure

Compound	$-J/k$ (K)	g	Cu—Cu distance (Å)	Ref.
$Cu(ap)_2 \cdot 4\ H_2O$	151, 185 [a]	2.06, 2.10	2.949	98, 99, 20
$Cu(ap)_2 \cdot 3\ H_2O$	156	2.07		100
$CuCl_2(apH)_2 \cdot 3/2\ H_2O$	206	2.15	3.066 [b]	100, 23
$CuBr_2(apH)_2 \cdot 2\ H_2O$	208	2.12		100
$CuCl_2(apH)$	44	2.10		100
$CuCl_2(hpH)_2 \cdot H_2O$	200	2.11	3.024 [b]	100, 24
$CuBr_2(hpH)_2 \cdot 2\ H_2O$	206	2.13		100
$CuCl_2(hpH) \cdot H_2O$	104	2.12		100
$CuBr_2(hpH) \cdot 1/2\ H_2O$	134	2.07		100
$Cu(az)_2 \cdot 2\ DMSO$	280 [a]	2.11		99
$Cu(CH_3COO)_2(azH)$	230 [a]	2.15		99
$Cu(CH_3COO)(az)(azH)$	167 [a]	2.11		99
$Cu(CH_3COO)(az)(C_5H_5N)$	196 [a]	2.12		99
$Cu(CH_3COO)_2 \cdot H_2O$	204	2.13	2.64, 2.556	104, 16, 17

[a] The values are reported in cm^{-1} in ref. 99.

[b] The crystal analyses were carried out on trihydrates.

According to the mechanism of the direct exchange interaction, the absolute value of exchange integral increases with decreasing metal—metal distance in a dimeric unit. However, Table 5 shows that the J-value has no correlation to the Cu—Cu distance. Comparison between copper(II) complexes of acetate and formate also shows the absence of any correlation between the J-value and the Cu—Cu distance [101,102]. For example, copper(II) formate monourea exhibits a stronger magnetic interaction (effective magnetic moment, 1.08 B.M.) than does copper(II) acetate monohydrate (1.40 B.M.) [103,104], whereas the formate has a longer Cu—Cu distance (2.657 Å) than that in the acetate (2.556 Å) [17,101]. Goodgame et al. [102] have also obtained experimental evidence against the direct exchange interaction in binuclear copper(II) alkanoates, $[(CH_3)_4N][Cu(HCOO)_2(NCS)]$ and $[(CH_3)_4][Cu(CH_3COO)_2(NCS)]$, both of which have dimeric units, $[Cu_2(RCOO)_4(NCS)_2]$, analogous to that in copper(II) acetate monohydrate: the formate has a larger absolute J-value (J/k = —349 K) than that of the acetate (J/k = —220 K), whereas the former has a greater Cu—Cu separation (2.716 Å) than that of the latter (2.643 Å). Inoue and Kubo [105] recorded the PMR spectra of two different modifications of copper(II) formate and obtained direct experimental evidence for superexchange interaction through formate groups. The carbon atoms of formate groups carry negative spin density (—0.024) on the $p\pi$ orbital in the blue form exhibiting two-dimensional antiferromagnetism, while negative spin density (—0.023) is distributed on the σ orbital of the carbon atoms in the royal blue form displaying ferromagnetism. Zelonka and Baird [106] observed the PMR spectrum of copper(II) benzoate in acetone solution, and concluded spin delocalization in a benzene ring and hence the predominance of superexchange mechanism. Taking these experimental results into account, we can conclude that magnetic interaction is dominated by superexchange mechanism in the copper(II) complexes of purine derivatives also, although the effect of direct exchange interaction is not entirely negligible [100].

Brookes and Martin [99,107,108] have determined the magnetic susceptibility of the nickel(II), copper(II), and cobalt(II) complexes of 7-azaindole. The formation of dimeric units is suspected for diamagnetic $Ni(az)_2$ from mass spectra [107]. The magnetic susceptibility of $Cu(az)_2 \cdot 2$ DMSO (DMSO: dimethylsulfoxide) has been explained by eqn. (2) over a temperature range of 80—300 K [99]. The formation of binuclear clusters has been confirmed for $Cu(CH_3COO)_2(azH)$, $Cu(CH_3COO)(az)(azH)$, and $Cu(CH_3COO)_2(azH)(pyridine)$ by the variation of magnetic susceptibility in the temperature range of 80—300 K; the g- and J-values are given in Table 5. For a cobalt(II) complex, $Co_4O(az)_6$, a very interesting structure has been conceived; four cobalt atoms are arranged tetrahedrally about an oxygen atom and are bridged by azaindolate ions to form a tetranuclear cluster. The dependence of magnetic susceptibility on temperature (80—500 K) has been analyzed successfully with a theoretical equation for tetramers consisting of spins $S = 3/2$, and yielded $J = -16\ \mathrm{cm}^{-1}$ or $J/k = -23$ K.

Sacconi et al. [27] measured the magnetic susceptibility of a nickel complex of 1,8-naphthyridine, $[Ni_2Br_2(1,8\text{-nph})_4] \cdot B(C_6H_5)_4$, in which nickel is formally 1.5-valent. At room temperature, the effective magnetic moment is equal to 4.19 B.M. per molecule of the chemical formula, a value which is close to the spin-only moment, 3.87 B.M., for $S = 3/2$. In the temperature range of 85—300 K, susceptibility obeys the Curie—Weiss law, yielding a Weiss constant equal to —3 K. The authors presume that the three highest levels of the ten molecular orbitals formed from the *d* orbitals of two nickel atoms have almost the same energy, and hence three unpaired electrons in these levels have parallel spins in accordance with the Hund rule. Magnetic moments have been determined at room temperature for various metal complexes of 1,8-naphthyridine having a normal central metal valency: $Co(NO_3)_2$-$(1,8\text{-nph})_2$ (effective magnetic moment, 4.60 B.M.), $Ni(NO_3)_2(1,8\text{-nph})_2$ (3.23 B.M.), $NiBr_2(1,8\text{-nph})_2$ (3.18 B.M.), and $Cu(NO_3)_2(1,8\text{-nph})_2$ (1.98 B.M.) [27,109]. The magnetic susceptibility of $CuCl_2(1,8\text{-nph})$ and $CuBr_2(1,8\text{-nph})$ can be explained by eqn. (2) for binuclear clusters in a temperature range of 80—300 K, the exchange integral being equal to $-70\ cm^{-1}$ ($J/k = -100$ K) and $-114\ cm^{-1}$ ($J/k = -164$ K) for the chloride and bromide complexes, respectively [110]. Because the exchange integral depends on the kind of halide ions, bridging by halide ions is conceivable, whereas 1,8-naphthyridine is coordinated to copper as an endobidentate ligand.

REFERENCES

1 J.A.J. Jarvis, Acta Crystallogr., 15 (1962) 964.
2 C.W. Reimann and M. Zocchi, Chem. Commun., (1968) 272.
3 J.A.J. Jarvis and A.F. Wells, Acta Crystallogr., 13 (1960) 1027.
4 H.C. Freeman, Adv. Protein Chem., 22 (1967) 257.
5 G. Ivarsson, B.K.S. Lundberg and N. Ingri, Acta Chem. Scand., 26 (1972) 3005.
6 B.K.S. Lundberg, Acta Chem. Scand., 26 (1972) 3902.
7 A.B.P. Lever, J. Lewis and R.S. Nyholm, Nature (London), 189 (1961) 58.
8 A.B.P. Lever, J. Lewis and R.S. Nyholm., J. Chem. Soc., (1962) 1235.
9 A.B.P. Lever, J. Lewis and R.S. Nyholm., J. Chem. Soc., (1963) 5042.
10 J.D. Dunitz, Acta Crystallogr., 10 (1957) 307.
11 P.J. Clarke and H.J. Milledge, Acta Crystallogr., Sect. B, 31 (1975) 1543.
12 F.D. Ayres, P. Pauling and G.B. Robertson, Inorg. Chem., 3 (1964) 1303.
13 A. Santoro, A.D. Mighell and C.W. Reimann, Acta Crystallogr., Sect. B, 26 (1970) 979.
14 R.C.E. Belford, D.E. Fenton and M.R. Truter, J. Chem. Soc., Dalton Trans., (1974) 17.
15 B. Morosin, R.C. Hughes and Z.G. Soos, Acta Crystallogr., Sect. B, 31 (1975) 762.
16 J.N. van Niekerk and F.R.L. Schoening, Acta Crystallogr., 6 (1953) 227.
17 R. Chidambaram and G.M. Brown, Cryst. Struct. Commun., 1 (1972) 269.
18 P.W. Carreck, M. Goldstein, E.M. McPartlin and W.D. Unsworth, Chem. Commun., (1971) 1634.
19 T. Asakawa, M. Inoue and M. Kubo, unpublished work.
20 E. Sletten, Acta Crystallogr., Sect. B, 25 (1969) 1480.
21 A. Terzis, A.L. Beauchamp and R. Rivest, Inorg. Chem., 12 (1973) 1166.
22 P. de Meester, D.M.L. Goodgame, P.K. Angela and A.G. Skapski, Nature (London), 229 (1971) 191.

23 P. de Meester and A.C. Skapski, J. Chem. Soc. A, (1971) 2167.
24 E. Sletten, Acta Crystallogr., Sect. B, 26 (1970) 1609.
25 P. de Meester and A.C. Skapski, J. Chem. Soc., Dalton Trans., (1972) 2400.
26 P. de Meester and A.C. Skapski, J. Chem. Soc., Dalton Trans., (1973) 424.
27 L. Sacconi, C. Mealli and D. Gatteschi, Inorg. Chem., 13 (1974) 1985; D. Gatteschi, C. Mealli and L. Sacconi, J. Am. Chem. Soc., 95 (1973) 2736.
28 J.S. Smart, in G.T. Rado and H. Suhl (Eds.), Magnetism, Vol. 3, Academic Press, New York and London, 1963, p. 63.
29 E. Sinn, Coord. Chem. Rev., 5 (1970) 313.
30 M. Inoue, M. Kishita and M. Kubo, Inorg. Chem., 6 (1967) 900.
31 K. Hara, M. Inoue, S. Emori and M. Kubo, J. Magn. Reson., 4 (1971) 337.
32 M.E. Lines, A.P. Ginsberg, R.L. Martin and R.C. Sherwood, J. Chem. Phys., 57 (1972) 1
33 S. Emori, T. Tokii and Y. Muto, Bull. Chem. Soc. Jpn., 48 (1975) 1649.
34 M.E. Fisher, J. Math. Phys. (N.Y.), 4 (1963) 124.
35 J.C. Bonner and M.E. Fisher, Phys. Rev., 135 (1964) A640.
36 M.E. Fisher, Am. J. Phys., 32 (1964) 343.
37 T. Smith and S.A. Friedberg, Phys. Rev., 176 (1968) 660.
38 W. Duffy, Jr. and K.P. Barr, Phys. Rev., 165 (1968) 647.
39 Z.G. Soos, J. Chem. Phys., 43 (1965) 1121.
40 M. Inoue and M. Kubo, J. Magn. Reson., 4 (1971) 175.
41 Z.G. Soos, Ann. Rev. Phys. Chem., 25 (1974) 121.
42 J.S. Smart, Effective Field Theories of Magnetism, Saunders, Philadelphia and London, 1966.
43 G.S. Rushbrooke and P.J. Wood, Mol. Phys., 1 (1958) 257.
44 C. Domb, in G.T. Rado and Suhl (Eds.), Magnetism, Vol. 2A, Academic Press, New York and London, 1965, p. 1.
45 S. Kadota, I. Yamada, S. Yoneyama and K. Hirakawa, J. Phys. Soc. Jpn., 23 (1967) 751.
46 J.B. Goodenough, Magnetism and the Chemical Bond, Wiley, New York and London, 1963.
47 J. Kanamori, J. Phys. Chem. Solids, 10 (1959) 87.
48 A.P. Ginsberg, Inorg. Chim. Acta, Rev., (1971) 45.
49 D.R. Eaton and W.D. Phillips, Adv. Magn. Reson., 1 (1965) 103.
50 G.N. LaMar, W. DeW. Horrocks, Jr. and R.H. Holm (Eds.), NMR of Paramagnetic Molecules, Academic Press, New York and London, 1973.
51 H.M. McConnell and D.B. Chesnut, J. Chem. Phys., 28 (1958) 107.
52 H.M. McConnell and R.E. Robertson, J. Chem. Phys., 29 (1958) 1361.
53 T.H. Brown, D.H. Anderson and H.S. Gutowsky, J. Chem. Phys., 33 (1960) 720.
54 T.R. Tuttle and S.I. Weissmann, J. Am. Chem. Soc., 80 (1958) 5342.
55 B.L. Barton and G.K. Fraenkel, J. Chem. Phys., 41 (1964) 1455.
56 S. Emori, M. Inoue and M. Kubo, Bull. Chem. Soc. Jpn., 45 (1972) 2259.
57 K. Hyde, G.F. Kokoszka and G. Gordon, J. Inorg. Nucl. Chem., 31 (1969) 1993.
58 J.E. Andrew, P.W. Ball and A.B. Blake, Chem. Commun., (1969) 143.
59 A.B.P. Lever, L.K. Thompson and W.M. Reiff, Inorg. Chem., 11 (1972) 104; R.L. Carlin and J.N. McElearney, Inorg. Chem., 11 (1972) 2291; A.B.P. Lever, L.K. Thompson and W.M. Reiff, Inorg. Chem., 11 (1972) 2292.
60 D.B. Losee, H.W. Richardson and W.E. Hatfield, J. Chem. Phys., 59 (1973) 3600.
61 R.J. Dudley, R.J. Fereday, B.J. Hathawa, P.G. Hodgson and P.C. Power, J. Chem. Soc., Dalton Trans., (1973) 1044.
62 M. Inoue, S. Emori, K. Hara and M. Kubo, J. Magn. Reson., 17 (1975) 212.
63 K. Takeda, S. Matsukawa and T. Haseda, J. Phys. Soc. Jpn., 30 (1971) 1330.
64 D.Y. Jeter and W.E. Hatfield, J. Inorg. Nucl. Chem., 34 (1972) 3055.
65 H.W. Richardson, W.E. Hatfield, H.J. Stoklosa and J.R. Wasson, Inorg. Chem., 12 (1973) 2051.

66 H.J. Stoklosa, J.R. Wasson, E.V. Brown, H.W. Richardson and W.E. Hatfield, Inorg. Chem., 14 (1975) 2378.
67 H.W. Richardson and W.E. Hatfield, J. Am. Chem. Soc., 98 (1976) 835.
68 M.J.M. Campbell, R. Grzeskowiak and F.B. Taylor, J. Chem. Soc. A, (1970) 19.
69 G.W. Inman, Jr. and W.E. Hatfield, Inorg. Chem., 11 (1972) 3085.
70 R.P. Eckberg and W.E. Hatfield, J. Chem. Soc., Dalton Trans., (1975) 616.
71 A.E. Underhill, J. Chem. Soc., (1965) 4336.
72 D.E. Billing, A.E. Underhill, D.M. Adams and D.M. Morris, J. Chem. Soc. A, (1966) 902.
73 D.E. Billing and A.E. Underhill, J. Inorg. Nucl. Chem., 30 (1968) 2147.
74 J.S. Valentine, A.J. Silverstein and Z.G. Soos, J. Am. Chem. Soc., 96 (1974) 97.
75 M. Goldstein, F.B. Taylor and W.D. Unsworth, J. Chem. Soc., Dalton Trans., (1972) 418.
76 R.W. Matthews and R.A. Walton, Inorg. Chem., 10 (1971) 1433.
77 D.E. Billing and A.E. Underhill, J. Chem. Soc. A, (1968) 5.
78 D.E. Billing, A.E. Underhill and G.M. Smart, J. Chem. Soc. A, (1968) 8.
79 G. Beech and C.T. Mortimer, J. Chem. Soc., (1967) 1115.
80 F. Cariati, D. Galizzioli, F. Morazzoni and L. Naldini, Inorg. Nucl. Chem. Lett., 9 (1973) 743.
81 E.B. Fleischer, D. Jeter and R. Florian, Inorg. Chem., 13 (1974) 1042.
82 S. Trofimenko, Chem. Rev., 72 (1972) 497.
83 M. Inoue, M. Kishita and M. Kubo, Inorg. Chem., 4 (1965) 626.
84 R. Robson, Aust. J. Chem., 23 (1970) 2217.
85 D. Nicholls and B.A. Worburton, J. Inorg. Nucl. Chem., 33 (1971) 1041.
86 W.D. McFadyen, R. Robson and H. Schaap, Inorg. Chem., 11 (1972) 1777.
87 M. Inoue and M. Kubo, J. Coord. Chem., submitted.
88 G.P. Brown and S. Aftergut, J. Polym. Sci., Part A, 2 (1964) 1839.
89 J.E. Bauman and J.C. Wang, Inorg. Chem., 3 (1964) 368.
90 W.J. Eilbeck, F. Holmes and A.E. Underhill, J. Chem. Soc. A, (1967) 757.
91 W.J. Eilbeck, F. Holmes, C.E. Taylor and A.E. Underhill, J. Chem. Soc. A, (1968) 128.
92 D.M.L. Goodgame, M. Goodgame, P.J. Hayward and G.W. Rayner-Canham, Inorg. Chem., 7 (1968) 2447.
93 M.E. Bridson and W.R. Walker, Aust. J. Chem., 23 (1970) 1973.
94 E. Baraniak, H.C. Freeman and C.E. Nockolds, J. Chem. Soc. A, (1970) 2558.
95 I.A. Cohen and D. Ostfeld, ACS Symp. Ser., 5 (1974) 221.
96 M. Inoue, S. Emori and M. Kubo, Inorg. Chem., 7 (1968) 1427.
97 M. Inoue and M. Kubo, Inorg. Chem., 5 (1966) 70.
98 D.M.L. Goodgame and K.A. Price, Nature (London), 220 (1968) 783.
99 R.W. Brookes and R.L. Martin, Inorg. Chem., 14 (1975) 528.
100 T. Asakawa, M. Inoue, K. Hara and M. Kubo, Bull. Chem. Soc. Jpn., 45 (1972) 1054.
101 D.B.W. Yawney and R.J. Doedens, Inorg. Chem., 9 (1970) 1626.
102 D.M.L. Goodgame, N.J. Hill, D.F. Marsham, A.C. Skapski, M.L. Smart and P.G.H. Troughton, Chem. Commun., (1969) 629.
103 M. Kishita, M. Inoue and M. Kubo, Inorg. Chem., 3 (1964) 237.
104 B.N. Figgis and R.L. Martin, J. Chem. Soc., (1956) 3837.
105 M. Inoue and M. Kubo, Inorg. Chem., 9 (1970) 2310.
106 R.A. Zelonka and M.C. Baird, Inorg. Chem., 11 (1972) 134.
107 R.W. Brookes and R.L. Martin, Aust. J. Chem., 27 (1974) 1569.
108 R.W. Brookes and R.L. Martin, Aust. J. Chem., 28 (1975) 1363.
109 D.G. Hendricker and R.J. Foster, Inorg. Chem., 12 (1973) 349.
110 K. Emerson, A. Emad, R.W. Brookes and R.L. Martin, Inorg. Chem., 12 (1973) 978.